

## Pressure dependence of argon cluster size for different nozzle geometries

Guanglong Chen,<sup>1</sup> Byunghoon Kim,<sup>1</sup> Byungnam Ahn,<sup>1,2</sup> and Dong Eon Kim<sup>1,a)</sup>

<sup>1</sup>Department of Physics, Pohang University of Science and Technology (POTTECH), Pohang 790-784, Republic of Korea

<sup>2</sup>Vacuum Measurement Technology, Pohang 790-320, Republic of Korea

(Received 4 April 2009; accepted 22 July 2009; published online 2 September 2009)

We experimentally study Rayleigh scattering from a cluster jet produced by high pressure argon gas expanding into vacuum through four different nozzles (a supersonic slit nozzle, a slit nozzle, a conical nozzle, and a sonic nozzle). The scattering signal intensity and the scattering image are recorded by photomultiplier tube and charge-coupled device camera, respectively. Based on the scattering image, the atom density in the gas flow is estimated. This allows for the comparison of the dependence of average cluster size on argon gas backing pressure between the nozzles. The experimental results show that the planar expansion developed from the supersonic slit and the slit nozzles exhibits the higher atom density than the axisymmetric expansion from the conical and the sonic nozzles. The slit nozzle is shown to have the highest pressure dependence of average cluster size. It is found that the supersonic slit nozzle is more favorable to the large clusters than the slit nozzle under the backing pressure of up to 50 bars, though it has the lower pressure dependence of average cluster size. © 2009 American Institute of Physics. [doi:10.1063/1.3204974]

### I. INTRODUCTION

Atomic clusters, a state of matter intermediate between molecules and solids, have been studied for many years since Becker *et al.*<sup>1</sup> first reported the cluster formation. For more than a decade, the interaction of intense femtosecond laser pulses with clusters has been an active area of research, and important findings have been reported: the generation of x rays, energetic ions and electrons,<sup>2-4</sup> and the intense femtosecond laser-driven nuclear fusion.<sup>5</sup> To understand the laser-cluster interaction, the size information of these weakly bound van der Waals clusters is required. The atomic clusters are usually formed in the adiabatic expansion of high pressure gas into vacuum through a nozzle. Hence the gas properties, source conditions, and the nozzle geometry affect the cluster formation and thus the properties of the cluster jet. However, the difficulty to describe the cluster formation has prevented a quantitative theory from being developed.<sup>6</sup> Experimentally, many methods have been developed to estimate the cluster size.<sup>6-12</sup> As a feasible approach, Rayleigh scattering measurement has been widely used.<sup>10-15</sup> From Rayleigh scattering measurement, however, the determination of absolute cluster size is not practical.<sup>11</sup> Traditionally, for the axisymmetric expansion of the rare gas, Hagena's scaling law  $N_c \sim (\Gamma^*)^{2.35}$  between the average atomic cluster size  $N_c$  (the number of atoms per cluster) and the Hagena's empirical parameter  $\Gamma^* (=Kd_{\text{eq}}^{0.85}P_0/T_0^{2.29})$  has served primarily as a guideline for the average cluster size, where  $K$  is a constant related to the gas property,  $P_0$  the gas backing pressure in mbar,  $T_0$  the gas temperature in kelvin before expansion, and  $d_{\text{eq}}$  the equivalent diameter of nozzle in  $\mu\text{m}$  [ $d_{\text{eq}} = 0.74d/\tan(\alpha)$  for a conical nozzle,  $d$  is the throat diameter of nozzle, and  $\alpha$  is the expansion half angle].<sup>6,16-18</sup> There have been many works that, using Rayleigh scattering from

the cluster jets, studied the pressure dependence of the scattering signal intensity  $S_{\text{RS}}$  for the axisymmetric expansion ( $S_{\text{RS}} \sim P_0^{2.6-3.6}$ ).<sup>8-13</sup> These experimental results revealed that the pressure dependence of the average cluster size is  $N_c \sim P_0^{1.6-2.6}$  under the assumption that all of the atoms are condensed into clusters. The results were roughly in agreement with the pressure dependence obtained from Hagena scaling law and confirmed that the scaling law could predict the pressure dependence of cluster size for the axisymmetric expansion.

However, so far, the experimental study on the scaling of  $S_{\text{RS}}$  or  $N_c$  with  $P_0$  for the planar expansion is scarce. Very recently, DeArmond *et al.*<sup>15</sup> reported their measurement of Rayleigh scattering from argon clusters formed in a planar expansion through a 15 cm long slit nozzle and found that the scattering signal exhibits the higher pressure dependence for the planar expansion than for the axisymmetric expansion.

In this paper, Rayleigh scattering method is employed to investigate the argon cluster formation from four nozzles with different geometries, i.e., the supersonic slit nozzle, the slit nozzle, the conical nozzle, and the sonic nozzle [a photomultiplier tube (PMT) and a charge-coupled device (CCD) camera are used to detect the scattering signal and image the scattered light, respectively]. Due to difficulties in the determination of absolute cluster size only from Rayleigh scattering measurement, this work assesses the pressure dependence of the relative cluster size for these nozzles. The spatial profiles of Rayleigh scattering signal from CCD image are used to estimate the cross section of gas flow and thus the atom density. It is shown that although the slit nozzle, corresponding to the planar expansion, exhibits the highest dependence of average cluster size on the gas backing pressure, the supersonic slit nozzle is more helpful to form large clusters under usual cluster experimental conditions.

<sup>a)</sup>Electronic mail: kimd@postech.ac.kr.

## II. DEPENDENCE OF CLUSTER SIZE

The Rayleigh scattering cross section for a spherical cluster is given by

$$\sigma \propto \frac{r^6}{\lambda^4} \left( \frac{i^2 - 1}{i^2 + 2} \right), \quad (1)$$

where  $r$  is the cluster radius,  $\lambda$  the wavelength of the laser, and  $i$  the refractive index of the cluster medium.<sup>10</sup> Since the average cluster size  $N_c$  is proportional to  $r^3$  for the spherical cluster,  $\sigma \propto N_c^2$ , Rayleigh scattering signal is then given by

$$S_{RS} \propto n_c \sigma \propto n_c N_c^2, \quad (2)$$

where  $n_c$  is the number of clusters in the scattering region. Under the assumption that all the atoms are condensed into clusters in the gas expansion, the number of clusters in the scattering region can be expressed as

$$n_c \propto nl/N_c, \quad (3)$$

for a given laser beam, where  $n$  is the atom number density in the scattering region and  $l$  is the dimension of the scattering region along the laser beam. Thus, Rayleigh scattering signal can be rewritten as

$$S_{RS} \propto n l N_c. \quad (4)$$

Using Eq. (4) and the experimental results about the pressure dependence of Rayleigh scattering signal  $S_{RS} \propto (P_0)^\beta$ , the relation between the average cluster size  $N_c$  and the gas backing pressure  $P_0$  can be expressed as

$$N_c \propto S_{RS}/nl \propto (P_0)^\beta/nl. \quad (5)$$

For a stable gas flow, at a distance of a few nozzle-orifice diameters downstream, the flow velocity  $v$  reaches its final value  $[\gamma/(\gamma-1)]^{1/2}(2kT_0/m)^{1/2}$ , where  $\gamma$  is the specific heat ratio,  $k$  is the Boltzmann constant, and  $m$  is the atomic mass.<sup>18,19</sup> From the continuity equation,

$$n_0 v_0 A_0 = n v A, \quad (6)$$

where  $n_0$ ,  $v_0 = (2kT_0/m)^{1/2}$ , and  $A_0$  are the atom number density, the flow velocity, and the area of the gas flow at the nozzle throat, respectively, and  $n$ ,  $v$ , and  $A$  are the respective values in the scattering region;<sup>18</sup> the average cluster size for a given backing pressure  $P_0$  can be expressed as

$$N_c \propto S_{RS} A / (n_0 A_0 l). \quad (7)$$

Because  $n_0$  is proportional to  $P_0$  and  $A_0$  is the same ( $A_0 = \pi d^2/4$ ) for the different nozzles, i.e., the area of the 0.5 mm diameter orifice in the pulsed valve in our work, the average cluster size can also be given by

$$N_c \propto S_{RS} A / (P_0 l). \quad (8)$$

## III. EXPERIMENTS

The experimental setup is shown in Fig. 1(a). A pulsed valve (Parker series 99) with a 0.5 mm diameter orifice is used. The 0.5 mm diameter orifice shown in Fig. 1(b) is itself used as a sonic nozzle. The other nozzles shown in Fig. 1(b) are directly placed on the top of the 0.5 mm diameter orifice. The slit width of the slit nozzle and the supersonic slit nozzle

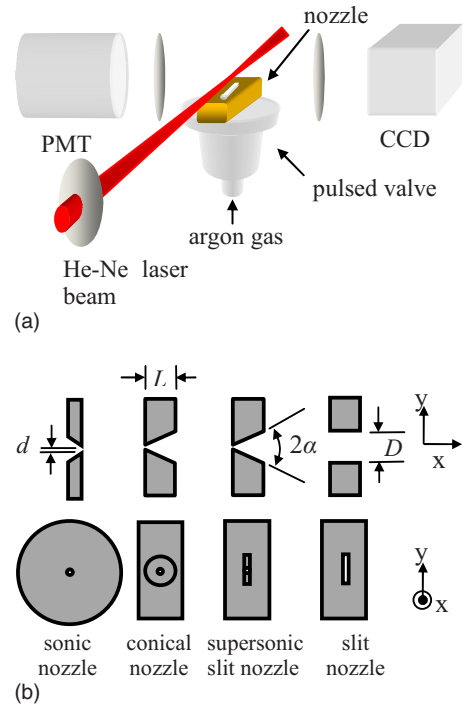


FIG. 1. (Color online) Schematic diagram of (a) experimental setup and (b) nozzle geometries ( $d=0.5$  mm,  $D=5.0$  mm,  $L=5.0$  mm, and the sonic nozzle is made of stainless steel and the others are made of brass). The upper and the lower figures in (b) are the side cross-sectional view and the top view of the nozzles, respectively.

is 0.5 mm. The supersonic slit, the slit, and the conical nozzles have the same dimension for nozzle exit,  $D$ . The half opening angle for the supersonic slit and the conical nozzles is  $24.2^\circ$ . In our experiment, the repetition rate of the pulsed valve is set to be  $1/12$  Hz, and the pressure of  $3 \times 10^{-5}$  Torr is maintained before the operation of the pulsed valve using turbo molecular pumps (Balzers TPH330). Argon clusters are produced in the adiabatic expansion of high pressure argon gas through one of these nozzles into vacuum. The He-Ne laser (UNIPHASE 1125, 632.8 nm and 10 mW) beam is focused by a lens with a 20 cm focal length and passes through the argon gas flow perpendicularly at 2.5 mm above from the nozzle exit, as shown in Fig. 1(a). The laser beam diameter in the gas jet is estimated to be less than 1 mm. Care is taken to reduce background lights from the vacuum chamber ( $59 \times 53 \times 30$  cm<sup>3</sup>) walls as much as possible. For the slit nozzle and the supersonic slit nozzle, the laser beam propagates along the slit direction. A 2 in. diameter lens with a 7.5 cm focal length is mounted about 19 cm away from the laser beam and is used to collect and image the  $90^\circ$  Rayleigh scattering light onto a head-on type PMT ( $-1$  kV is applied). The axis of the lens is mutually perpendicular to the laser beam and the gas jet. The output signal from the PMT is recorded by a 1 GHz bandwidth digital oscilloscope (Tektronix TDS5104). Meanwhile, a CCD camera located at the opposite side of the PMT is used to image the  $90^\circ$  Rayleigh scattering light from the cluster jet. Note that the collection solid angle subtended by the optical system described above is large enough to cover all the scattering regions for different nozzles, and one optical setup is used for different nozzles.

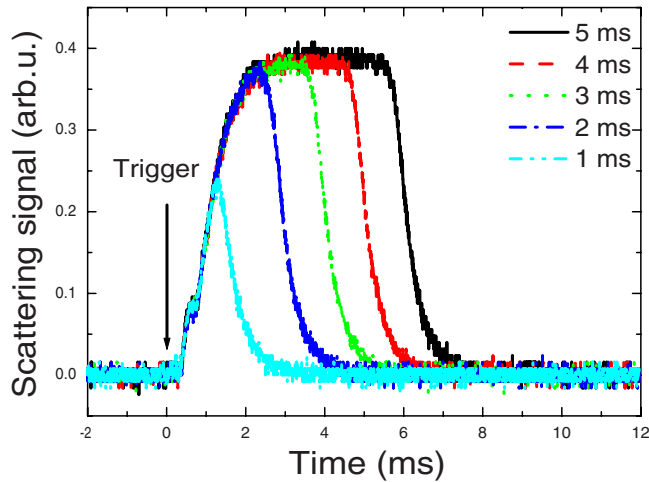
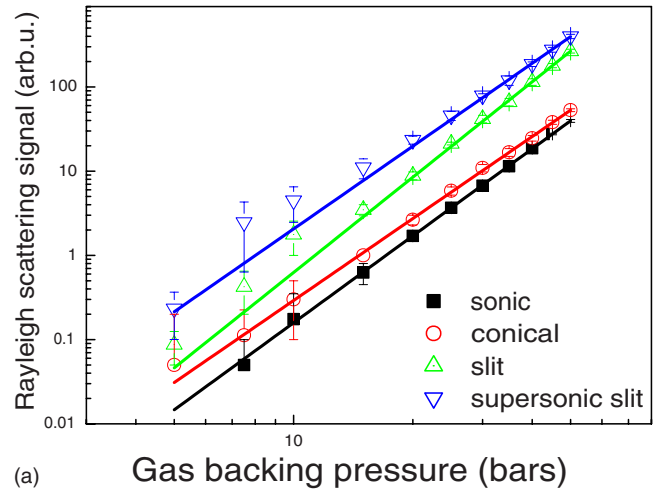


FIG. 2. (Color online) Time-resolved Rayleigh scattering signal from PMT at a backing pressure of 50 bars (argon gas) for the supersonic slit nozzle for different valve opening times.

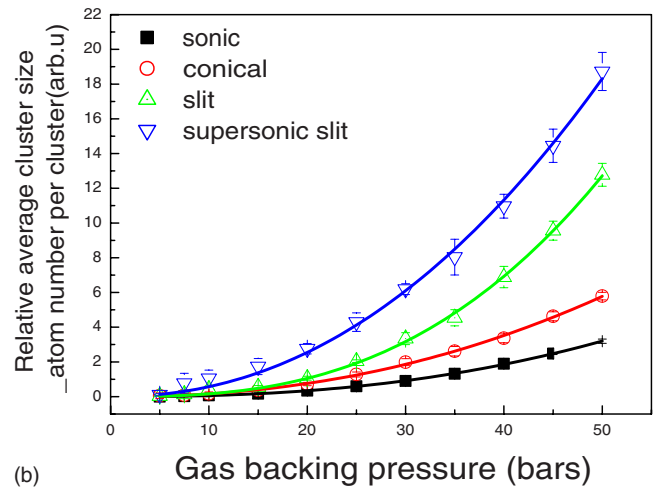
#### IV. RESULTS AND DISCUSSION

First, to adjust the valve opening time and guarantee the steady state gas flow, which is critical to the cluster formation, the time-resolved Rayleigh scattering measurement at a gas backing pressure of 50 bars was performed for the supersonic slit nozzle. Figure 2 is the scattering signal recorded by the PMT for different valve opening times, showing that Rayleigh scattering signal reaches the steady state and has the flat top profiles when the pulsed valve opening time is longer than 3 ms. These data imply that both gas flow and cluster formation thus reach the steady state when the valve opening time is not less than 3 ms under our experimental conditions. It was also true for other nozzles. All the experiment data were obtained at the valve opening time of 3 ms, unless otherwise mentioned, and were quite reproducible.

The dependence of the Rayleigh scattering signal  $S_{RS}$  and the average cluster size  $N_c$  on the gas backing pressure for different nozzles is shown in Fig. 3. Every data point was obtained by averaging 40 gas pulses. Figure 3(a) indicates that the scattering signal  $S_{RS}$  for the supersonic slit and the slit nozzles is much higher than that for the conical and the sonic nozzles. Furthermore, for the planar gas expansion, the supersonic slit nozzle demonstrates the higher scattering signal than the slit nozzle, and for the axisymmetric gas expansion, the scattering signal for the supersonic nozzle (conical nozzle) is higher than that for the sonic nozzle. By fitting  $S_{RS} \sim (P_0)^\beta$  to the scattering signal, we obtain  $\beta$  of  $3.27 \pm 0.17$ ,  $3.76 \pm 0.16$ ,  $3.24 \pm 0.19$ , and  $3.43 \pm 0.12$  for the supersonic slit, the slit, the conical, and the sonic nozzles, respectively. The power  $\beta$  for the conical and the sonic nozzles (corresponding to the axisymmetric expansion) are close to the previous measurements.<sup>10-15</sup> Furthermore, it is found that the pressure dependence of 3.76 for the slit nozzle is higher than that for other nozzles. This indicates that for the planar expansion developed through the slit nozzle, the pressure dependence of scattering signal is different from that for the axisymmetric expansion. This is in agreement with the result by DeArmond,<sup>15</sup> where the pressure dependence between a 15 cm long slit nozzle and a sonic nozzle



(a) Gas backing pressure (bars)



(b) Gas backing pressure (bars)

FIG. 3. (Color online) Pressure dependence of (a) Rayleigh scattering signal and (b) the average cluster size for different nozzles. The solid lines represent the fit to the data.

was compared. However, it is interesting to note that for the supersonic slit nozzle, the pressure dependence of scattering signal is lower than that for the slit nozzle and close to that for the conical nozzle. We have also investigated the pressure dependence of Rayleigh scattering signal at the different distances (from 1.5 to 3.5 mm) downstream from the nozzle exit and found that the change in  $\beta$  at the different distances is within  $\pm 4.5\%$ .

To compare the average size of clusters produced from the different nozzles, the information about the dimension  $l$  and the area  $A$  of the scattering region is required by Eq. (8). The CCD image from the scattered light was used to estimate the scattering dimension  $l$  and the scattering area  $A$  of the gas flow where the laser beam passed through. Figure 4 shows the typical CCD images at 2.5 mm away from the nozzle exit for different nozzles at a backing pressure of 50 bars. For the supersonic slit and the slit nozzles, to estimate the scattering area, the transverse image of the scattered light was also recorded after the slit direction was set to be perpendicular to the laser beam. Figures 4(b) and 4(d) are the scattering images of the gas flow along the slit direction, while Figs. 4(e) and 4(f) are the transverse images perpen-

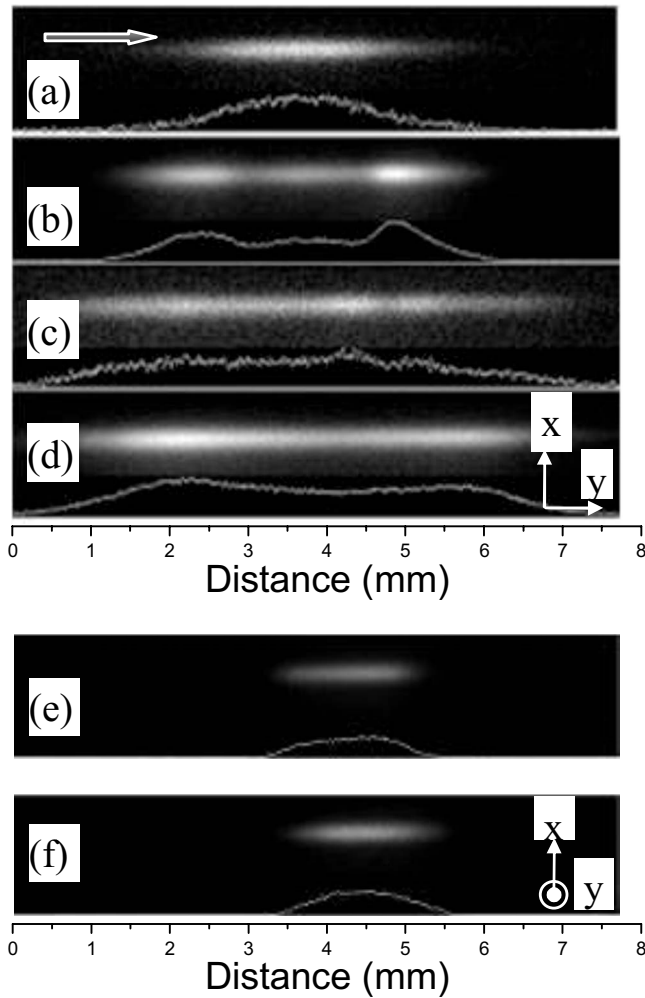


FIG. 4. CCD images of the scattered light for (a) the sonic, (b) the slit (along the slit direction), (c) the conical, and (d) the supersonic slit (along the slit direction) nozzles at an argon gas backing pressure of 50 bars. (e) and (f) are the transverse images (perpendicular to the slit direction) for the slit and the supersonic slit nozzles, respectively. The laser beam direction is shown as the arrow. Due to the weaker scattering signal for sonic and conical nozzles, images (a) and (c) were obtained at the valve opening time of 5 ms. (Note that the scales of signal intensity for the different nozzles are different.)

pendicular to the slit direction for the supersonic slit and the slit nozzles, respectively. It can be seen that for the slit or the supersonic slit nozzle, the dimension of gas flow perpendicular to the slit is much narrower than that along the slit. Thus we can think that the gas flow from the slit or the supersonic slit nozzle behaves like a planar expansion. The white curves in Fig. 4 show the profiles along the laser beam at the center of the image, i.e., the spatial distribution of the scattered light. It is found that these nozzles can produce the roughly uniform profile except for the sonic nozzle, and the gas expansion through the conical or the supersonic slit nozzle forms the wider gas flow, i.e., the gas flow with the larger dimension.

We define the dimension of the scattering region in the gas flow as the length of scattering region where the scattered light intensity is higher than 3% of the maximum intensity. This definition is based on the fact that the dimension of the scattering region estimated from the CCD image should be close to the slit length  $D$  (5.0 mm) due to the zero

expansion angle for the slit nozzle. Considering the difference in the scattered light intensity for different nozzles, we first normalized the spatial intensity profile of the scattered light. The dimension  $l$  was then taken at the 3% level in the normalized profile and estimated to be 7.3, 5.0, 7.0, and 5.2 mm for the supersonic slit, the slit, the conical, and the sonic nozzles, respectively. For the axisymmetric expansion (the sonic and the conical nozzles), the area of the scattering region  $A$  can be obtained immediately using  $\pi l^2/4$ . For the planar expansion (the supersonic slit and the slit nozzles), the required transverse dimensions of the scattering region are estimated to be about 2.4 mm from the transverse images. Then we estimate the scattering area  $A$  at a backing pressure of 50 bars to be 17.1, 12.0, 38.0, and 20.8 mm<sup>2</sup> for the supersonic slit, the slit, the conical, and the sonic nozzles, respectively. Based on Eq. (6) and the estimated areas  $A$ , the ratios of the corresponding atom number density in the scattering region among these nozzles are given by 2.2:3.2:1.0:1.8 at a backing pressure of 50 bars for the supersonic slit, the slit, the conical, and the sonic nozzles, respectively. Clearly, the gas flows from the supersonic slit and the slit nozzles have higher atom density due to the slit geometry. It is interesting to note that for the sonic nozzle, atom density is higher than for the conical nozzle in our work. The reason is discussed below. For the sonic nozzle, the scattering region is at 2.5 mm above from the nozzle exit, i.e., 2.5 mm above the orifice in the pulsed valve. While for the conical nozzle, although the scattering region is also at 2.5 mm above from the conical nozzle exit, it is actually 7.5 mm above the orifice in the pulsed valve due to the nozzle length  $L$  [Fig. 1(b)]. Thus it is not surprising that the conical nozzle corresponds to lower atom density than the sonic nozzle. Note that the atom number density ratio between the slit and the sonic nozzles is much lower than that calculated by the equation in Table I in Ref. 18. This is understood because the slit configuration (the area of the gas flow at the nozzle throat  $A_0 = dD$ ) in Ref. 18 is different from our slit nozzle configuration ( $A_0$  is  $\pi d^2/4$ ).

After estimating the area of the scattering region  $A$  and the dimension of the scattering region  $l$ , we use Rayleigh scattering signal  $S_{RS}$  to calculate the relative average cluster sizes for different nozzles at a backing pressure of 50 bars using Eq. (8). If we use the  $A$  and  $l$  at the 50 bars pressure for the lower backing pressures, the relative cluster sizes at the lower backing pressures can be obtained, as shown in Fig. 3(b). By fitting these relative cluster sizes to the pressure power dependence of  $N_c \sim (P_0)^B$ ,  $B$  was estimated to be  $2.16 \pm 0.11$ ,  $2.73 \pm 0.10$ ,  $2.23 \pm 0.13$ , and  $2.45 \pm 0.10$  (only including the uncertainty in Rayleigh scattering signal) for the supersonic slit, the slit, the conical, and the sonic nozzles, respectively. Note that for the axisymmetric gas expansion, the conical nozzle corresponds to lower pressure dependence than the sonic nozzle. As in the pressure dependence of Rayleigh scattering signal, the pressure dependence of average cluster size is the highest for the slit nozzle. Moreover the pressure dependence of average cluster size for the supersonic slit nozzle is close to that for the conical nozzle. Although at present it is not easy to explain this result due to the lack of theory, we think that the reason for the fact that

the pressure dependence for the supersonic slit nozzle is lower than that for the slit nozzle could result from different expansion angle. Unlike the slit nozzle, which has a zero opening expansion angle [ $\alpha=0$  in Fig. 1(b)], the opening expansion angle of supersonic slit nozzle can make the gas expansion along the  $y$  direction. This can be seen from Fig. 4, where the length of scattering region ( $y$  direction) is longer than the length of nozzle exit for the supersonic slit nozzle, while the length of scattering region is close to the length of nozzle exit for the slit nozzle. Thus the gas expansion from the supersonic slit nozzle is different from that from the slit nozzle (mainly along  $x$  direction) but is similar to a 2 dimensional expansion (not only along  $x$  but also along the  $y$  direction).

Note that the high pressure dependence of cluster size (large  $B$ ) only means a fast increasing trend in the cluster size with the backing pressure. As shown in Fig. 3(b), although the conical nozzle corresponds to the lower pressure dependence, the relative average cluster size for the conical nozzle is estimated to be 1.8 times larger than that for the sonic nozzle at a backing pressure of 50 bars. This is in agreement with the fact that the supersonic geometry of conical nozzle is helpful for the large cluster formation for the axisymmetric gas expansion.<sup>6</sup> To further understand the result, we quantitatively compare the relative average cluster size for the conical nozzle with that for the sonic nozzle using Hagen scaling law.<sup>6</sup> From the equivalent diameter model,<sup>18</sup> the equivalent diameter of the conical nozzle [ $d_{eq}=0.74d/\tan(\alpha)$ ] is about 1.64 times larger than that of the sonic nozzle. Thus the average cluster size is about 2.6 times larger than that for the sonic nozzle based on Hagen scaling law  $N_c \sim (\Gamma^*)^B$  ( $B=2.23$  for our experimental results). This result is roughly in agreement with our estimated value (1.8) from the experiment data. The deviation could result from the assumption in the equivalent diameter model that the streamline of the flow field is straight. Based on this model, the dimension of the scattering region at 2.5 mm downstream from the nozzle exit for the conical nozzle is about 7.3 mm, while the estimated dimension from the CCD image is 7.0 mm. The other possible reason is that, as discussed above, the distances between the scattering region and the orifice in the pulsed valve are different for the sonic and the conical nozzles, while the average cluster size could be related to the distance.<sup>12</sup>

Figure 3(b) shows that for given gas source conditions, the average cluster size for the supersonic slit nozzle is the largest in our work. The average cluster size is about 1.5 times larger than that produced from the slit nozzle at backing pressure of 50 bars. Specifically, if, as practiced by others,<sup>13–15</sup> we take the cluster size  $N_c$  to be 100 atoms per cluster when the scattering signal is first detectable (the signal was first detected at 5 bars for the supersonic slit nozzle in our case), the average cluster size  $N_c$  at backing pressure of 50 bars is estimated to be about 14 000 ( $r=5.4$  nm) atoms per cluster using the pressure dependence of  $(P_0)^{2.16}$ . However for the slit nozzle, the average cluster size  $N_c$  at a backing pressure of 50 bars is estimated to be 9600 atoms ( $r=4.7$  nm) based on the relative cluster size shown in Fig. 3(b). These results could indicate that similarly to the axi-

symmetric gas expansion, the supersonic geometry of the supersonic slit nozzle is also helpful for the larger cluster formation.

It is interesting to find from Fig. 3(b) that the average cluster size produced from the slit nozzle is larger than that from the conical nozzle at a higher gas backing pressure. For example, the relative cluster size for the slit nozzle is larger than that for the conical nozzle by a factor of 2.2 at a backing pressure of 50 bars. The reason for this could result from the higher atom density in the gas flow for the slit nozzle as shown above. In our work, the conical nozzle has an exit whose diameter (5 mm) is equal to the slit length of the slit nozzle and thus has a large half opening angle of  $24.2^\circ$ . If a conical nozzle with a smaller opening angle is used, which can produce the gas jet with the same atom density as that from the present slit nozzle under a given backing pressure, the average cluster size from the conical nozzle could be expected to be larger than that from the slit nozzle due to supersonic geometry of the conical nozzle as discussed above.

## V. CONCLUSIONS

Using the scattered light intensity measurement by a PMT together with the scattered light image by a CCD, the pressure dependence of relative average cluster size has been investigated for an argon cluster jet developed from supersonic slit, slit, conical, and sonic nozzles. It is shown that the planar expansion developed from the supersonic slit and the slit nozzles exhibits the higher atom density than the axisymmetric expansion, and the slit nozzle corresponds to the highest pressure dependence of average cluster size. For the supersonic slit nozzle, unlike the slit nozzle, the pressure dependence is close to that for a conical nozzle. As known in axisymmetric gas expansion for the conical nozzle, it is found that although the supersonic slit nozzle has the lower pressure dependence than the slit nozzle, its supersonic geometry is still helpful in the case of a slit geometry for the formation of large clusters under the usual experimental conditions. The detailed comparison of average cluster size (not the pressure dependence of cluster size) between a slit nozzle and a conical nozzle with different half opening angles would be the interesting subjects for further work.

## ACKNOWLEDGMENTS

This work has been supported by BK21 project, Basic Research Program (Grant No. K12F-2008-313-C00356) funded by Korean Research Foundation, and Global Research Laboratory Program of the National Research Foundation.

<sup>1</sup>E. W. Becker, K. Bier, and W. Henkes, *Z. Phys.* **146**, 133 (1956).

<sup>2</sup>A. McPherson, B. D. Thompson, A. B. Borisov, K. Boyer, and C. K. Rhodes, *Nature (London)* **370**, 631 (1994).

<sup>3</sup>M. Lezius, S. Dobosz, D. Normand, and M. Schmidt, *J. Phys. B* **30**, L251 (1997).

<sup>4</sup>J. W. G. Tisch, T. Ditmire, D. J. Fraser, N. Hay, M. B. Mason, E. Sprin-gate, J. P. Marangos, and M. H. R. Hutchinson, *J. Phys. B* **30**, L709 (1997).

<sup>5</sup>T. Ditmire, J. Zweiback, V. P. Yanovsky, T. E. Cowan, G. Hays, and K. B. Wharton, *Nature (London)* **398**, 489 (1999).

- <sup>6</sup>O. F. Hagen and W. Obert, *J. Chem. Phys.* **56**, 1793 (1972).
- <sup>7</sup>M. Lewerenz, B. Schilling, and J. P. Toennies, *Chem. Phys. Lett.* **206**, 381 (1993).
- <sup>8</sup>R. Karnbach, M. Joppien, J. Stapelfeldt, and J. Wormer, *Rev. Sci. Instrum.* **64**, 2838 (1993).
- <sup>9</sup>K. Y. Kim, V. Kumarappan, and H. M. Michberg, *Appl. Phys. Lett.* **83**, 3210 (2003).
- <sup>10</sup>A. J. Bell, J. M. Mestdagh, J. Berlande, X. Biquard, J. Cuvelier, A. Lallement, P. Meynadier, O. Sublemontier, and J.-P. Visticot, *J. Phys. D* **26**, 994 (1993).
- <sup>11</sup>A. M. Bush, A. J. Bell, J. G. Frey, and J.-M. Mestdagh, *J. Phys. Chem. A* **102**, 6457 (1998).
- <sup>12</sup>A. Ramos, J. M. Fernández, G. Tejada, and S. Montero, *Phys. Rev. A* **72**, 053204 (2005).
- <sup>13</sup>R. A. Smith, T. Ditmire, and J. W. G. Tisch, *Rev. Sci. Instrum.* **69**, 3798 (1998).
- <sup>14</sup>B. Liu, P. Zhu, S. Li, G. Ni, and Z. Xu, *Chin. Phys. Lett.* **19**, 659 (2002).
- <sup>15</sup>F. M. DeArmond, J. Suelzer, and M. F. Masters, *J. Appl. Phys.* **103**, 093509 (2008).
- <sup>16</sup>O. F. Hagen, *Z. Phys. D: At., Mol. Clusters* **4**, 291 (1987).
- <sup>17</sup>O. F. Hagen, *Rev. Sci. Instrum.* **63**, 2374 (1992).
- <sup>18</sup>O. F. Hagen, *Surf. Sci.* **106**, 101 (1981).
- <sup>19</sup>K. L. Saenger, *J. Chem. Phys.* **75**, 2467 (1981).